© The American Society of Gene & Cell Therapy

Development of Novel Activin-Targeted Therapeutics

Justin L Chen[1,2,6], Kelly L Walton[1], Sara L Al-Musawi[1], Emily K Kelly[1], Hongwei Qian[2], Mylinh La[3], Louis Lu[3], George Lovrecz[3], Mark Ziemann[2], Ross Lazarus[2], Assam El-Osta[2], Paul Gregorevic[2,4,5,6] and Craig A Harrison[1,7,8]

[1]MIMR-PHI Institute of Medical Research, Clayton, Australia; [2]Baker IDI Heart and Diabetes Institute, Melbourne, Australia; [3]NCRIS Facility, CSIRO Material Sciences and Engineering, Clayton, Australia; [4]Department of Neurology, The University of Washington School of Medicine, Seattle, WA, USA; [5]Department of Physiology, The University of Melbourne, Melbourne, Australia; [6]Department of Biochemistry and Molecular Biology, Monash University, Clayton, Australia; [7]Department of Physiology, Monash University, Clayton, Australia; [8]Department of Molecular and Translational Sciences, Monash University, Clayton, Australia.

Soluble activin type II receptors (ActRIIA/ActRIIB), via binding to diverse TGF-β proteins, can increase muscle and bone mass, correct anemia or protect against diet-induced obesity. While exciting, these multiple actions of soluble ActRIIA/IIB limit their therapeutic potential and highlight the need for new reagents that target specific ActRIIA/IIB ligands. Here, we modified the activin A and activin B prodomains, regions required for mature growth factor synthesis, to generate specific activin antagonists. Initially, the prodomains were fused to the Fc region of mouse IgG2A antibody and, subsequently, "fastener" residues (Lys[45], Tyr[96], His[97], and Ala[98]; activin A numbering) that confer latency to other TGF-β proteins were incorporated. For the activin A prodomain, these modifications generated a reagent that potently (IC_{50} 5 nmol/l) and specifically inhibited activin A signaling *in vitro*, and activin A-induced muscle wasting *in vivo*. Interestingly, the modified activin B prodomain inhibited both activin A and B signaling *in vitro* (IC_{50} ~2 nmol/l) and *in vivo*, suggesting it could serve as a general activin antagonist. Importantly, unlike soluble ActRIIA/IIB, the modified prodomains did not inhibit myostatin or GDF-11 activity. To underscore the therapeutic utility of specifically antagonising activin signaling, we demonstrate that the modified activin prodomains promote significant increases in muscle mass.

Received 5 August 2014; accepted 9 November 2014; advance online publication 9 December 2014. doi:10.1038/mt.2014.221

INTRODUCTION

Activin type II receptors (ActRIIA/ActRIIB) mediate the signaling of a subset of transforming growth factor-β (TGF-β) ligands, including activin A, activin B, myostatin, and GDF-11.[1] Ligand binding to ActRIIA/IIB leads to the activation of type I receptors (ALK4, 5, or 7), which initiate an intracellular signaling cascade centred on Smad2/3 transcription factors.[2] Smad2/3 activation drives the expression of genes involved in cellular proliferation, differentiation, apoptosis and extracellular matrix deposition,[3] and is critical for the maintenance of adult tissue homeostasis. Accordingly, pharmacological blockade of the ActRIIA/IIB signaling pathway offers great potential to restore homeostasis in disease-affected tissues.

To date, ligand traps consisting of the extracellular domains of human ActRIIA or ActRIIB fused to IgG Fc regions have proven the most efficacious therapeutic reagents.[4–9] Soluble ActRIIA increases bone mass and strength and prevents cancer-induced bone destruction in models of myeloma and breast cancer,[5,8] by antagonising local activin A signaling. Interestingly, by inhibiting GDF-11, soluble ActRIIA also improves ineffective erythropoiesis and corrects anemia in a mouse model of β-thalassemia.[10] Soluble ActRIIB has even broader therapeutic potential, as it not only mimics the effects of soluble ActRIIA on bone growth and erythropoiesis,[7,9] but also dramatically increases muscle mass, predominantly by antagonizing myostatin activity.[4] As such, soluble ActRIIB has been used variously to improve muscle mass and function in the *mdx* mouse model of Duchenne muscular dystrophy,[11] and to reverse muscle wasting and prolong survival in murine models of cancer cachexia.[12] Recently, the potential of targeting the ActRIIA/IIB pathway to induce skeletal muscle hypertrophy has been confirmed using a human anti-ActRIIA/IIB antibody.[13] Surprisingly, this reagent also increased the mass and thermogenic activity of brown adipose tissue.[14]

Although, individually, these studies demonstrate the therapeutic potential of inhibiting the ActRIIA/IIB pathway, collectively they highlight problems associated with using ligand traps that target multiple TGF-β proteins. Thus, there is a growing acceptance that interventions that target either one, or a small subset, of ActRIIA/IIB ligands will be the most effective way to achieve a desired outcome (*e.g.*, muscle growth) with minimum risk of incurring significant off-target effects. In support, development of a modified soluble ActRIIB with negligible activin binding was recently shown to inhibit GDF-11 activity and promote erythropoiesis in mice.[9]

The first two and the last two authors contributed equally.

Correspondence: Paul Gregorevic, Baker IDI Heart and Diabetes Institute, P.O. Box 6492, St. Kilda Rd. Central, Melbourne 8008, Australia.
E-mail: paul.gregorevic@bakeridi.edu.au

© The American Society of Gene & Cell Therapy

Previously, we have shown that similar specificity for activins can be achieved by modifying the prodomain of activin A.[1] Like all TGF-β proteins, activin A is synthesized as a large precursor molecule with the N-terminal prodomain mediating the folding of the C-terminal mature domain.[15] Following processing and secretion, the prodomain remains noncovalently associated with activin A; however, the affinity of the interaction is not sufficient to suppress biological activity.[16,17] In contrast, TGF-β1, myostatin and GDF-11 bind their prodomains with high affinity and are secreted from the cell in a latent form.[18–20] By linking the N-terminal region of the activin A prodomain to the C-terminal region of the TGF-β1 prodomain, we generated a reagent that could antagonize activin A and B, but had low affinity for myostatin and GDF-11.[1]

Subsequently, the crystal structure of pro-TGF-β1 was solved.[21] The structure indicated that TGF-β1 is secreted in a latent form due to covalent dimerization of prodomain chains and the presence of "fastener" residues (Lys^{27}, Tyr^{74}, Tyr^{75}, Ala^{76}, and Arg^{238}), which tightly link various prodomain regions together. In this study, we modified the activin A and activin B prodomains to mimic the adaptions that confer latency to TGF-β1 and myostatin. The increased potency, specificity and stability of the resultant activin antagonists suggests that these reagents could be utilized to block pathogenic activin signaling in conditions such as cancer cachexia.[12]

RESULTS

Modification of the activin A and activin B prodomains

The prodomains of TGF-β family proteins can be expressed independently and retain the capacity to recomplex with their respective mature growth factors.[22–24] We produced the activin A, activin B, TGF-β1, and myostatin prodomains and assessed their inhibitory activity and specificity *in vitro* (see **Supplementary Figures 1** and **2** for complete amino acid sequences of all proteins used in this study). The wild-type activin prodomains were very poor antagonists of activin A and B signaling (**Supplementary Figure 3a**), indicating that they are readily displaced in the presence of ActRIIA/IIB. In contrast, the biological activity of TGF-β1 and myostatin was fully suppressed by their respective prodomains (**Supplementary Figure 3a**). Interestingly, the TGF-β1 prodomain not only antagonized TGF-β1 signaling, but also potently inhibited TGF-β2, TGF-β3, myostatin, and GDF-11 activity (**Supplementary Figure 3b**). The recently solved crystal structure of pro-TGF-β1 (**Figure 1a**)[21] indicates that the C-terminal portion of the α_1 prodomain helix forms the primary contacts with the mature growth factor. This region of the TGF-β1 prodomain (**Figure 1c**, underlined) is highly conserved in the prodomains of TGF-β2, TGF-β3, myostatin, and GDF-11, which explains why the TGF-β1 prodomain can bind and inhibit the activity of these other growth factors. The prodomains of activin A and activin B (and most other TGF-β proteins) are sufficiently distinct across the α_1 helix region (**Figure 1c**) to suggest that they may only bind to their mature growth factors. Thus, these prodomains could be developed as specific antagonists, if their affinity for activin A and activin B could be enhanced.

The crystal structure of pro-TGF-β1 (**Figure 1a**),[21] together with earlier studies,[17] identified two regions of the prodomain that confer latency to the mature growth factor: (i) cysteine residues (Cys^{223} and Cys^{225}) towards the C-terminus that covalently link prodomain chains and (ii) "fastener" residues (Lys^{27}, Tyr^{74}, Tyr^{75}, Ala^{76} and Arg^{238}), which tightly link various prodomain regions together and are highly conserved in other latent TGF-β proteins (**Figure 1b,c**). These two features of latent TGF-β proteins were incorporated into the activin A and activin B prodomains. Specifically, to covalently link activin prodomain chains, we generated fusion proteins with the Fc regions of mouse IgG2A. The Fc chains form covalent links, allowing the activin prodomains to dimerize. Second, to introduce a "fastener," we substituted residues in the activin A (Asn^{44}-Met^{45}; Ile^{87}-Glu^{102}) and activin B (Ile^{83}-Glu^{102}) prodomains with the corresponding myostatin prodomain residues (Ser^{39}-Lys^{40}; Asp^{87}-Thr^{94}) (**Figure 1c**, boxed residues). We chose to incorporate the myostatin fastener residues, rather than those from TGF-β1, because the myostatin and activin prodomains are more highly conserved in the surrounding regions. Together, these modifications dramatically increased affinity of the activin prodomains for activin A or activin B >100-fold (**Figure 1d,e**).

The modified activin prodomains are potent and specific activin antagonists

The modified activin A and activin B prodomains were assessed for their ability to suppress ActRIIA/IIB-mediated release of follicle stimulating hormone (FSH) by LβT2 pituitary gonadotrope cells. The modified activin A prodomain potently inhibited activin A signaling (IC_{50} 5 nmol/l), but displayed weak affinity for activin B (IC_{50} >100 nmol/l) and no inhibitory activity towards myostatin or GDF-11 (**Figure 2a**). Mechanistically, the modified activin A prodomain specifically blocked the ability of activin A to bind ActRIIA/IIB[1] and stimulate Smad2 phosphorylation (**Figure 2c**). Thus, the modified activin A prodomain represents the first example of a highly selective activin A antagonist. Interestingly, the modified activin B prodomain suppressed FSH release (**Figure 2b**) and Smad2 phosphorylation (**Figure 2d**) stimulated by both activin isoforms with similar potency (IC_{50} 1–3 nmol/l), but did not block myostatin or GDF-11 activity (**Figure 2b**). The modified activin B prodomain may, therefore, serve as a general activin antagonist.

The potencies of the prodomains relative to commonly used activin antagonists were also examined in the LβT2 cell assay system. The modified activin A prodomain (IC_{50} 5 nmol/l) was a less potent antagonist of activin A signaling than the activin B prodomain (IC_{50} 1.3 nmol/l), soluble ActRIIA (IC_{50} 0.8 nmol/l) or soluble ActRIIB (IC_{50} 2 nmol/l) (**Figure 2e**). However, this reduced potency would be compensated *in vivo* by the high specificity of this reagent. Similarly, the potency of the modified activin B prodomain to inhibit activin B signaling was three- to seven-fold lower than observed for soluble ActRIIA or soluble ActRIIB (**Figure 2f**), but far surpassed ActRIIA and ActRIIB in terms of ligand specificity.[1] Notably, in comparison to our first generation activin A antagonist,[1] the introduction of an Fc domain and fastener residues significantly increased potency (**Supplementary Figure 4**).

© The American Society of Gene & Cell Therapy

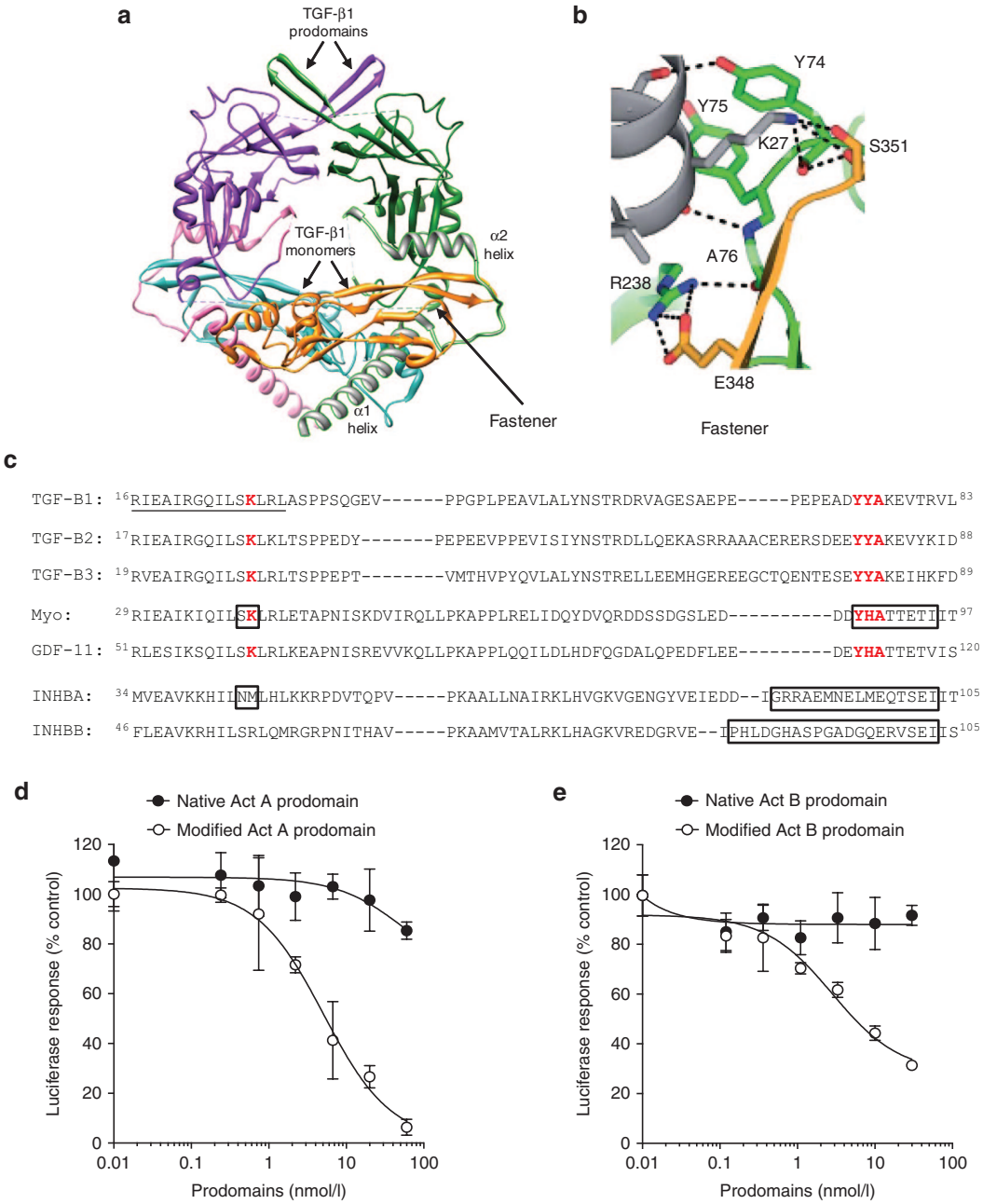

Figure 1 Generation of modified activin A and activin B prodomains. (**a**) Crystal structure of the mature TGF-β1 dimer (orange and turquoise) bound to its prodomain chains (green and purple) (PDB ID:3RJR).[21] Within this structure, the α_1 and α_2 helices of the prodomain form the primary contacts with the mature dimer. Adapted by permission from Macmillan Publishers Ltd: Nature,[21] copyright (2011). (**b**) The prodomain fastener is centred on Lys[27] in the α_1 helix, which forms a series of bonds/contacts with residues in the pro- (Tyr[74], Tyr[75] and Ala[76]) and mature (Ser[351]) domains. Reprinted by permission from Macmillan Publishers Ltd: Nature,[21] copyright (2011). (**c**) The fastener residues (*red*) are invariant among the TGF-β isoforms, and highly conserved in myostatin and GDF-11. Activin A and activin B lack an identifiable fastener. Nonfastener residues in the activin A and activin B prodomains (*boxed*) were substituted for the corresponding fastener residues from the myostatin prodomain (*boxed*). (**d**,**e**) Introduction of fastener residues and an Fc-tag dramatically increased the ability of the activin prodomains to block activin A- or activin B-induced stimulation of the Smad2/3-responsive A3-Lux luciferase reporter in HEK293T cells. Luciferase activity was measured and plotted as % control. Data are mean ± SD (n = 3) from a representative experiment.

Modified prodomains can specifically block activin-induced muscle wasting

We next assessed the ability of the modified prodomains to block activin A and B *in vivo* bioactivity. Recently, we demonstrated that adeno-associated viral vector (rAAV6) delivery of activin A or activin B gene expression constructs into the tibialis anterior (TA) muscles of wild-type mice caused profound muscle wasting and fibrosis.[25] These effects of activin A were associated with significant changes in gene expression (**Supplementary Table S1**) consistent with perturbation of signaling homeostasis, metabolic control, and the potentiation of pro-fibrotic markers. To determine if modified activin prodomains were protective, rAAV6

© The American Society of Gene & Cell Therapy

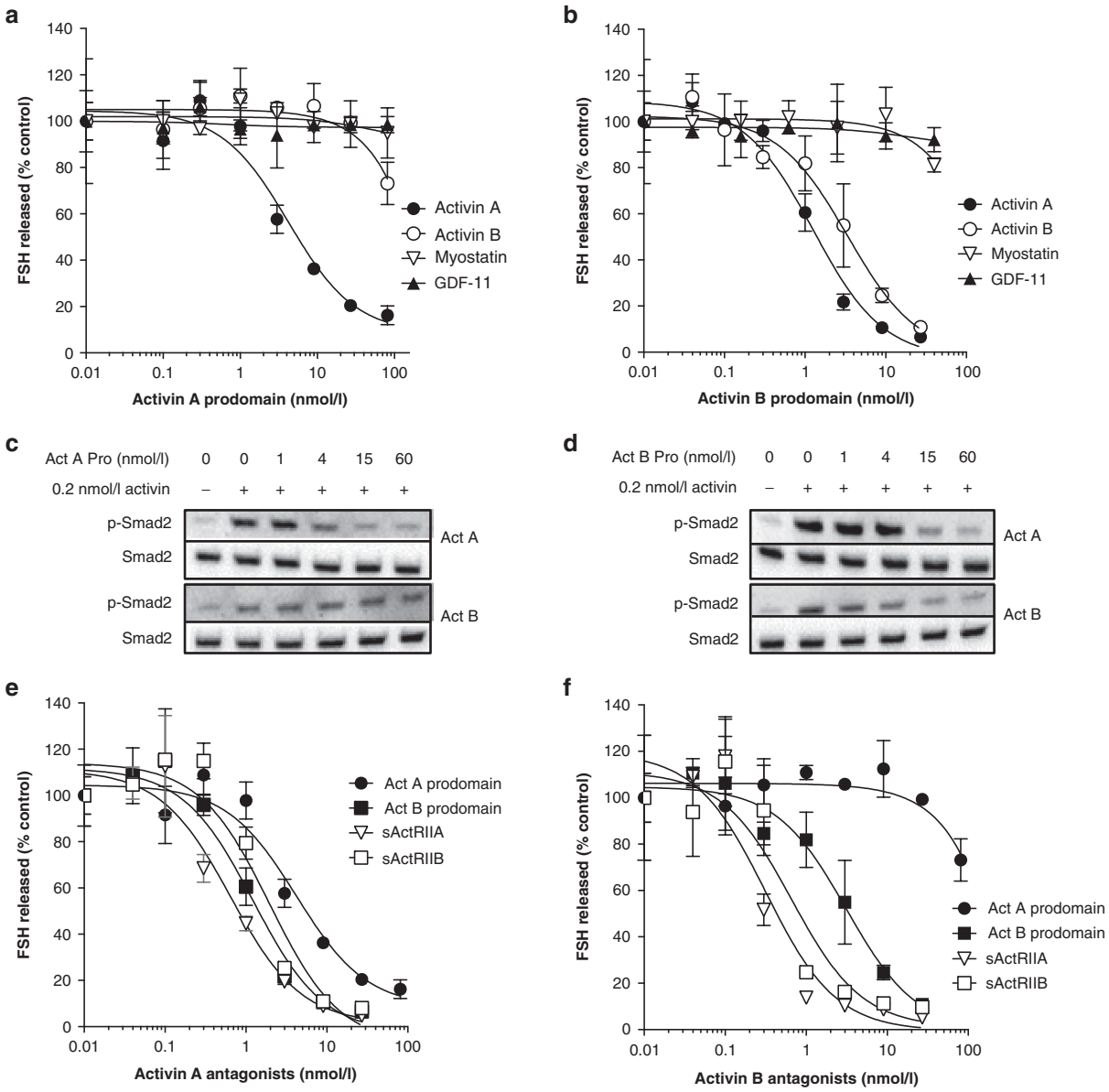

Figure 2 Modified activin prodomains are potent and specific activin A and B antagonists. LβT2 cells were stimulated with 0.2 nmol/l activin A, activin B, myostatin or GDF-11 in the absence or presence of increasing concentrations (0.01–100 nmol/l) of modified activin A prodomain (**a**) or modified activin B prodomain (**b**). FSH production was measured and plotted as % control (**a**,**b**), while the degree of Smad2 phosphorylation was determined by Western blot, using phosphor-Smad2 and total-Smad2 antibodies (**c**,**d**). To assess the potency of the modified activin prodomains, relative to soluble activin receptors, LβT2 cells were stimulated with 0.2 nmol/l activin A (**e**), or activin B (**f**), and treated with increasing doses of antagonists (0.01–100 nmol/l). FSH production was measured and plotted as % control. Data are mean ± SD from three representative experiments.

vectors encoding for activin A or activin B were delivered to muscles alone, or in combination with vectors that increased expression of the activin A or activin B prodomains. As anticipated, 4 weeks after rAAV6:activin A delivery into TA muscles, significant muscle atrophy was observed (33% decrease; **Figure 3a**). Codelivery of rAAV6:activin A with rAAV6:activin A prodomain or rAAV6:activin B prodomain not only prevented this loss of muscle mass, but led to mass increases of 8 and 17%, respectively, compared to the mass of control TA muscles, which received rAAV6:control vector (**Figure 3a**). Expression of activin A and B prodomain was confirmed in treated TA muscles by Western blot for FLAG (**Figure 3b**), and qRT-PCR indicated that the presence of the modified prodomains did not affect activin A mRNA levels (**Figure 3c**). Hematoxylin and eosin-stained cryosections revealed smaller muscle fibers within TA muscles injected with rAAV6:activin A alone. However, muscle fiber size was preserved in muscles coexpressing modified activin A or activin B prodomain, with activin A (**Figure 3d**,**e**). Mechanistically, the modified prodomains blocked activin A's ability to bind to its signaling receptors[1] and stimulate phosphorylation of Smad3 in TA muscles (**Figure 3f**). Suppression of Smad3 phosphorylation was accompanied by a significant reduction in the expression of activin A-induced atrophy-related genes, including *Igfn1* and *Mss51* (**Figure 4a**). As activin A can promote fibrosis as well as cause atrophy in skeletal muscle,[25] we next sought to determine whether the

© The American Society of Gene & Cell Therapy

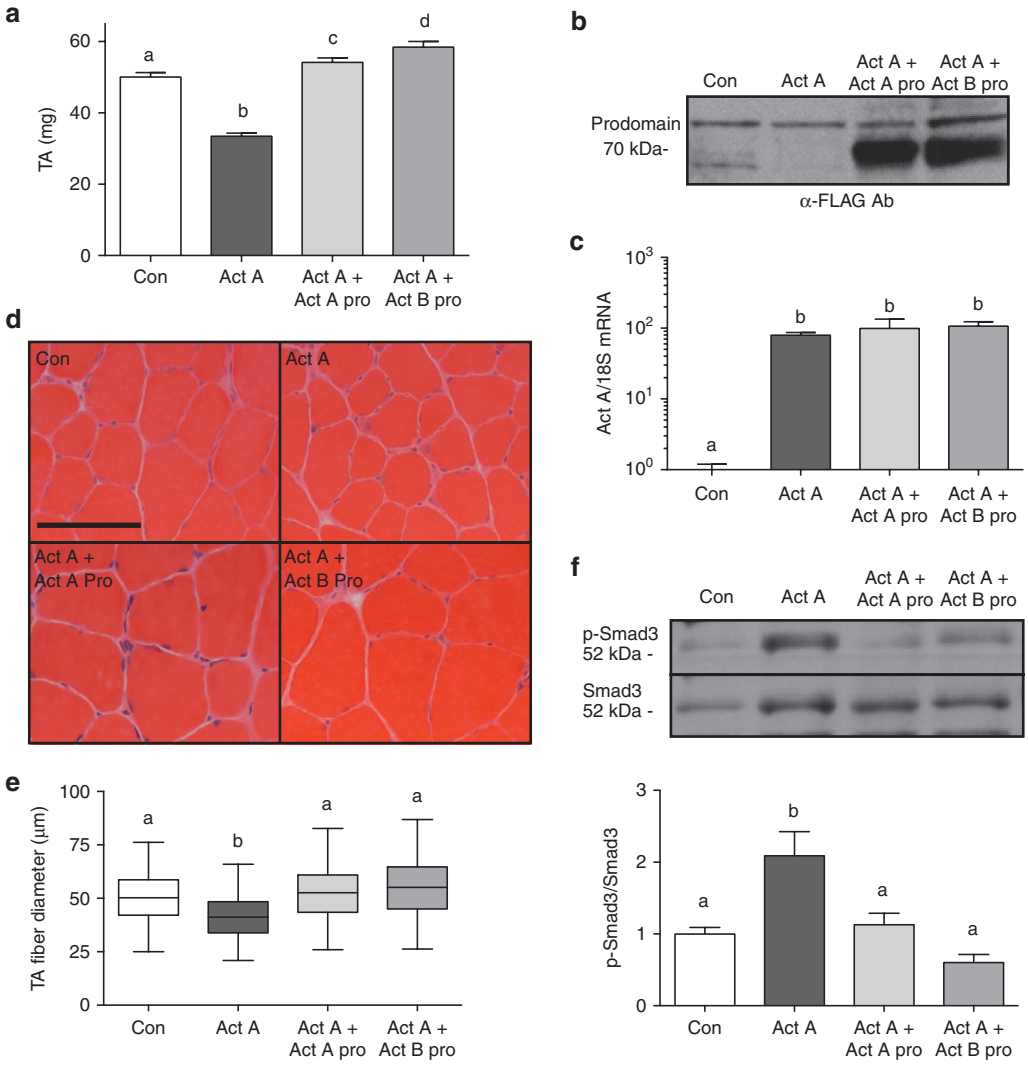

Figure 3 Activin A-induced muscle wasting is reversed by both the modified activin A and activin B prodomains. rAAV6:activin A (10^9 vector genomes. v.g.) was injected into the right TA muscle of C57BL/6 mice alone, or in combination with rAAV6:activin A prodomain or rAAV6:activin B prodomain (10^{10} v.g.). Four weeks after AAV injections, TA muscles were excised and weighed (**a**, n = 7 for Con, Act A, and Act A + Act B pro; n = 8 for Act A + Act A pro). In these muscles, the expression of prodomains (**b**) and activin A (**c**, n = 4 for Con and Act A + Act B pro; n = 3 for Act A and Act A + Act A pro) were assessed by Western blot and qRT-PCR, respectively. (**d**,**e**) Muscle atrophy in response to activin A and reversal following prodomain treatment, was a product of changes in muscle fiber size (reported here as representative hematoxylin and eosin-stained cryosections (**d**, bar = 100 μm), and a box and whisker plot (**e**, n = 3 for Con, Act A + Act A pro, and Act A + Act B Pro; n = 4 for Act A; at least 200 myofibers were counted per TA muscle) comprising minimum, lower quartile, median, upper quartile, and maximum values for myofiber diameter). (**f**) Western blot analysis of TA muscles 4 weeks after vector administration demonstrated that activin A-induced Smad3 phosphorylation was inhibited by the modified activin A and B prodomains (n = 7 for Con, Act A, and Act A + Act B pro; n = 3 for Act A + Act A pro).

modified activin prodomains also suppressed activin A-induced upregulation of genes associated with extracellular matrix deposition (**Supplementary Table S1**). In TA muscles treated with activin A, *Comp*, *Eln*, *Adamts8*, and *Mfap4* mRNA expression, quantified by qRT-PCR, increased 3- to 12-fold. However, the expression of modified activin A and B prodomains completely blocked the potentiation of these genes by activin A (**Figure 4b**). Thus, the ability of activin A to promote atrophy in muscle fibers and activate extracellular matrix deposition by myofibroblasts is completely inhibited by delivery of the modified activin A or activin B prodomains.

Consistent with our *in vitro* data (**Figure 2**), activin B-induced muscle wasting was only prevented with codelivery of the rAAV6:activin B prodomain (whereas the activin A prodomain had no effect; **Figure 5a**). This was not due to a lack of expression of the modified activin A prodomain, as it was present in TA muscles at levels comparable to the activin B prodomain (**Figure 5b**). Nor, did the presence of the activin A prodomain increase activin B mRNA expression within skeletal muscle (**Figure 5c**). Consistent with this evidence of specificity for activin A by the activin A prodomain, muscle fiber atrophy caused by overexpression of activin B was prevented by codelivery of rAAV6:activin B prodomain, but not rAAV6:activin A prodomain (**Figure 5d**,**e**). Mechanistically, only the activin B prodomain blocked activin B-induced Smad3 phosphorylation in TA muscles (**Figure 5f**).

© The American Society of Gene & Cell Therapy

Administration of activin inhibitors reveals endogenous activins regulate skeletal muscle mass

Recent studies suggest that activins may act in concert with myostatin to negatively regulate muscle mass,[26,27] especially in conditions of disease.[12] To determine whether endogenous activins have a role in regulating skeletal muscle mass after development, we utilized local injection of rAAV6 vectors encoding either modified activin A or activin B prodomains into the right TA muscles of wild-type and myostatin-deficient mice. Four weeks post-AAV injections, the activin A and activin B prodomains caused small (14 and 11%, respectively), but significant increases in TA muscle mass in wild-type mice (**Figure 6a**), indicating that endogenous activin A and B can negatively regulate muscle mass. Interestingly, in *Mstn*$^{-/-}$ mice, which already display a hypermuscular phenotype,[27] the modified activin A and B prodomains induced a proportionally greater increase in muscle mass (**Figure 6b**). In particular, rAAV6:activin B prodomain administration, which inhibits both activin A and activin B signaling, resulted in the greatest muscle hypertrophy (50% increase; **Figure 6b**). The expression of both activin A and activin B prodomains was confirmed by Western blot in the treated TA muscles only (**Figure 6c,d**). Hematoxylin and eosin staining of the prodomain-treated TA muscles demonstrated normal muscle architecture with larger fibers compared with muscles receiving control vector (**Figure 6e,f**). As activin A and activin B mRNA levels are low in skeletal muscle, and do not change following myostatin knockout (**Supplementary Figure 5**), we predict that circulating activin A and B contribute to the negative regulation of muscle mass. In support of this hypothesis, activin A (55 ± 12 pg/ml) and activin B (532 ± 182 pg/ml) are readily detectable in mouse serum.[28] Together, these results indicate that specifically blocking activin signaling can lead to a significant increase in muscle mass.

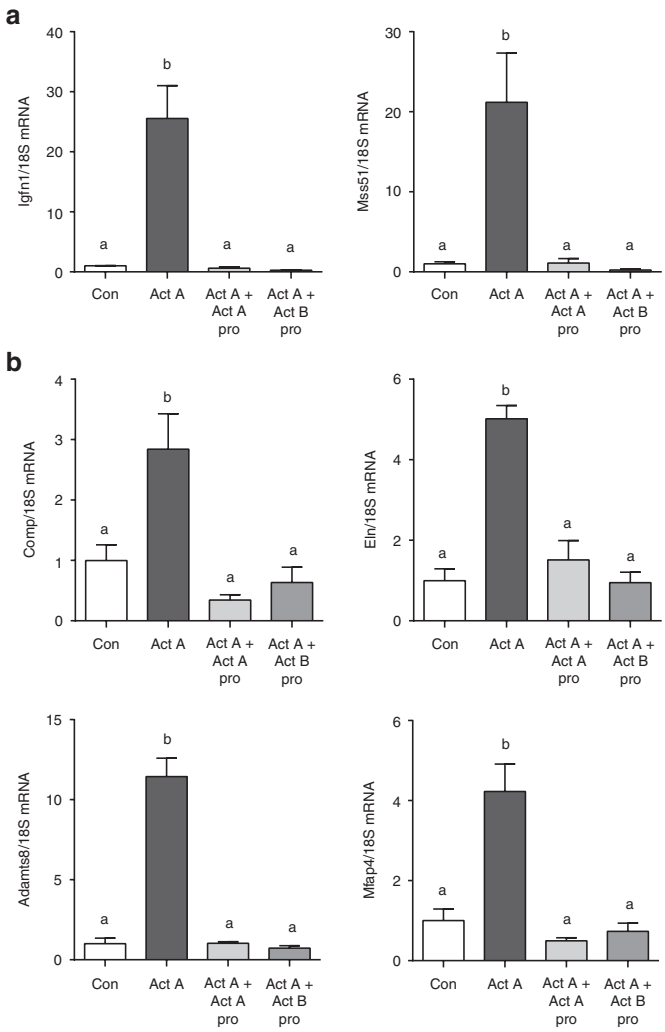

Figure 4 Activin A-induced increases in the expression of extracellular matrix and atrophy-related genes are blocked following prodomain treatment. qRT-PCR analysis of TA muscles examined 28 days after injection with rAAV6:activin A vector alone, or in combination with rAAV6:activin prodomain vectors. The increased transcription of atrophy-related (**a**) and extracellular matrix (**b**) genes induced by activin A was completely inhibited by the activin A and activin B prodomains (**a** and **b**; n = 4 for Con, Act A, and Act A + Act B pro; n = 3 for Act A + Act A pro).

DISCUSSION

Activin A and B are key autocrine/paracrine regulators of bone formation, reproduction, inflammation, metabolism and wound repair.[7,29–32] Recent animal studies have highlighted the therapeutic potential of specifically targeting the activin signaling pathway. First, activins appear to play a dominant role in the development and progression of the severe wasting syndrome cachexia.[12] In multiple cancer cachexia models, including colon-26 (C26) tumor-bearing mice and inhibin-deficient mice, activin A and B levels are dramatically elevated,[28] and we have shown that activins alone can induce the profound losses of skeletal muscle and fat mass that are key indicators of mortality in cachexia.[25] Importantly, blocking signaling by activin-related ligands in these cachexia models, using soluble ActRIIB, reverses muscle wasting and prolongs survival.[12] Second, endogenous activin A inhibits osteoblast differentiation and matrix mineralization and is, therefore, a potent negative regulator of bone growth.[7] Blocking activin A signaling, using soluble ActRIIA, increases bone formation and improves skeletal integrity in both normal mice and ovariectomized mice with established bone loss.[6,8] In addition, soluble ActRIIA treatment improves osteolytic disease and prolongs survival in mouse models of multiple myeloma.[5] While the ability of soluble activin type II receptors to block activin signaling and, thereby, reverse cachexia or promote bone growth is exciting, these reagents antagonize multiple TGF-β ligands, including specific BMPs that are associated with vascular remodeling.[25,33] Inhibiting the endogenous signaling of these other ligands may, in some cases, be contra-indicated.[34] On this basis, there is a significant need to develop effective, activin-specific interventions, with increased selectivity over soluble ActRIIA and ActRIIB.

As a strategy to develop improved activin inhibitors, we focused on understanding the mechanisms that underlie the synthesis, secretion and activation of activin-related proteins.[17,35–37] We have shown that the activin A and activin B prodomains template the correct folding and dimerization of their respective growth factors, and that extracellularly, prodomains stabilize mature activin dimers.[37] However, the affinity of prodomain binding to activin A or B is insufficient to inhibit biological activity.[1] In contrast, the TGF-β isoforms, myostatin and GDF-11 bind their

© The American Society of Gene & Cell Therapy

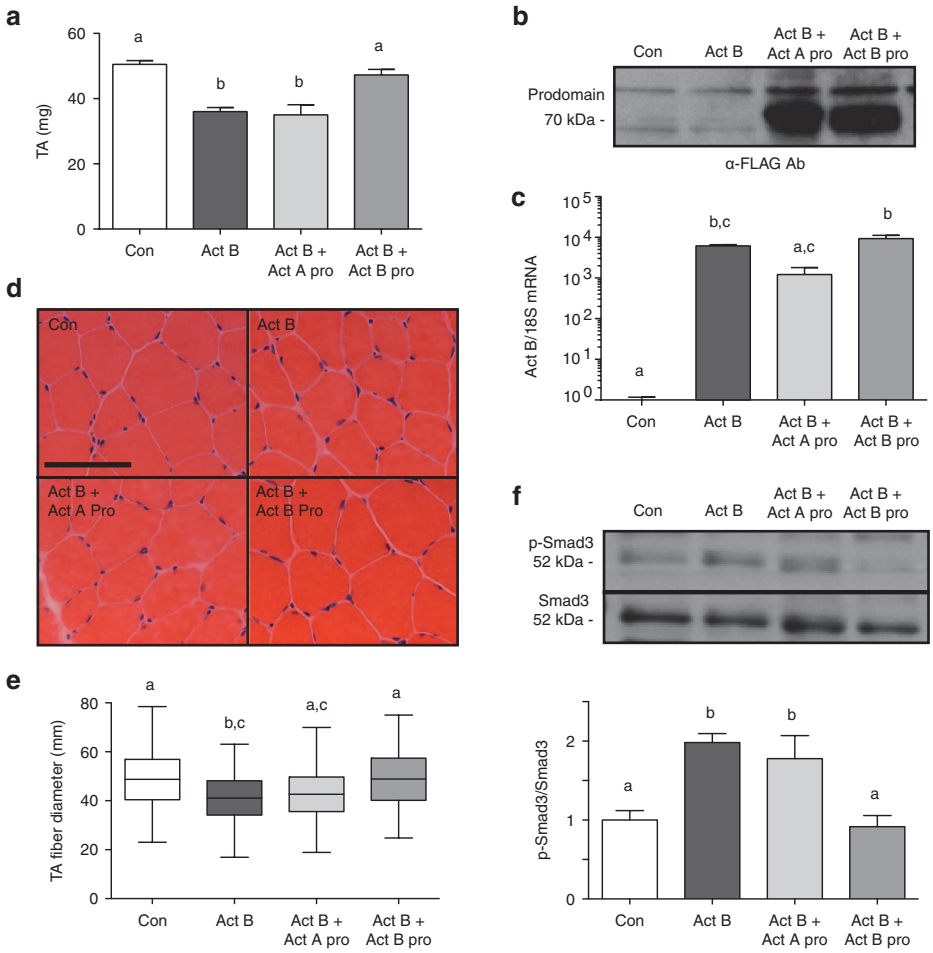

Figure 5 Activin B-induced muscle wasting is reversed by the modified activin B prodomain. rAAV6:activin B (10^9 v.g.) was injected into the right TA muscle of C57BL/6 mice alone, or in combination with rAAV6:activin A prodomain or rAAV6:activin B prodomain (10^{10} v.g.). Four weeks after AAV injections, TA muscles were excised and weighed (**a**, n = 10 for Con and Act B; n = 5 for Act B + Act A pro; n = 7 for Act B + Act B pro). In these muscles, the expression of prodomains (**b**) and activin B (**c**, n = 4 for Con, Act B, and Act B + Act B pro; n = 3 Act B + Act A pro) were assessed by Western blot and qRT-PCR, respectively. (**d**,**e**) Muscle atrophy in response to activin B and reversal following activin B prodomain treatment, was a product of changes in muscle fiber size (reported here as representative hematoxylin and eosin-stained cryosections (**d**, bar = 100 μm), and a box and whisker plot (**e** n = 3 for Con, Act B, and Act B + Act A pro; n = 4 for Act B + Act B pro; at least 200 myofibers were counted per TA muscle), comprising minimum, lower quartile, median, upper quartile, and maximum values for myofiber diameter). (**f**) Western blot analysis of TA muscles 4 weeks after vector administration demonstrated that activin B-induced Smad3 phosphorylation was only inhibited by the modified activin B prodomain (n = 9 for Con and Act B; n = 3 for Act B + Act A pro and Act B + Act B pro).

prodomains with high affinity and are secreted in a latent form.[18–20] This knowledge led to the development of our first activin antagonist, which was generated by fusing the N-terminus of the activin A prodomain to the C-terminus of the TGF-β1 prodomain. This reagent preferentially inhibited activin A, over activin B, and demonstrated low affinity for myostatin and GDF-11.[1] The subsequent resolution of the pro-TGF-β1 crystal structure[21] provided much more refined information regarding prodomain residues that confer latency to mature TGF-β1, and enabled us to develop more potent and specific activin antagonists.

Specifically, the pro-TGF-β1 crystal structure identified "fastener" residues, which link three separate regions of the prodomain (α_1 helix, β1 sheet, and α_5 helix) and effectively lock mature TGF-β1 in the latent complex.[21] As the prodomains of all TGF-β proteins are predicted to have a similar fold, we reasoned that the introduction of "fastener" residues into the activin A and activin B prodomains would increase affinity for their mature growth factors. Covalent dimerization of TGF-β1 prodomains also contributes to latency and to mimic this, we fused the activin A and activin B prodomains (with introduced fastener residues) to the Fc-region of mouse IgG2A antibody. The modified activin A prodomain specifically antagonized activin A signaling *in vitro* (IC_{50} 5 nmol/l), while displaying very low affinity for activin B and no binding to myostatin or GDF-11. Thus, the modified activin A prodomain represents the first specific activin A antagonist and, potentially, a reagent that could be used for the treatment of diseases with skeletal fragility. In support of a therapeutic role, we showed that rAAV6-mediated delivery of the modified activin A prodomain into skeletal muscle protected against activin A-induced wasting, but could not block atrophy driven by activin B.

The modified activin B prodomain inhibited both activin A (IC_{50} 1 nmol/l) and activin B (IC_{50} 3 nmol/l) activity *in vitro*, but showed negligible affinity for myostatin or GDF-11. In an attempt

© The American Society of Gene & Cell Therapy

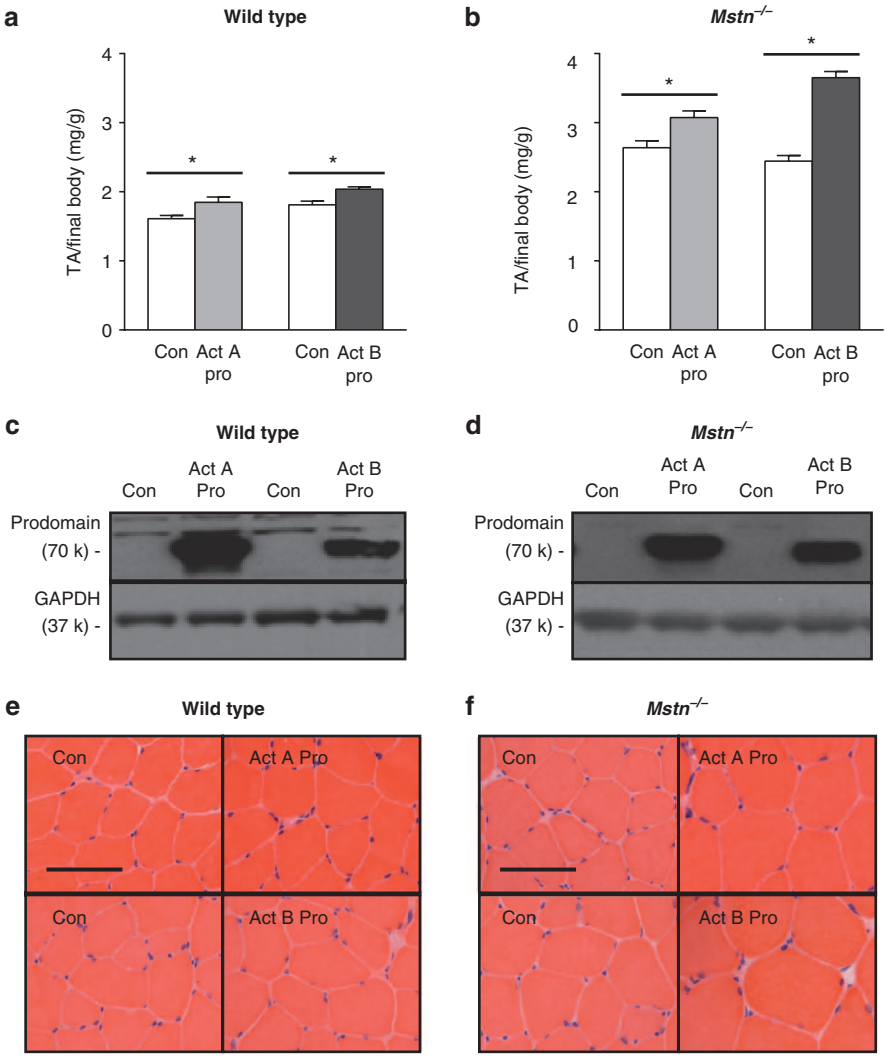

Figure 6 Activins contribute to the regulation of skeletal muscle mass. Right TA muscles of wild-type (**a**) and *Mstn*$^{-/-}$ (**b**) C57BL/6 mice were injected with rAAV6:activin A prodomain (1.5×10^{11} v.g.) or rAAV6:activin B prodomain (10^{10} v.g.), while the left TA muscles were injected with an equivalent dose of control vector. Four weeks after rAAV6 injections, TA muscles that were administered the prodomains increased in mass in both wild-type (**a**, n = 8 for Con and Act A pro; n = 5 for Con and Act B pro) and *Mstn*$^{-/-}$ (**b**, n = 7 for Con and Act A pro; n = 4 for Con and Act B pro) mice. (**c**,**d**) Western blot analysis confirmed expression of the prodomains in the treated TA muscles. (**e**,**f**) Muscle growth in response to prodomain treatment, was a product of increased fiber size (reported here as representative hematoxylin and eosin-stained cryosections), most notable in the *Mstn*$^{-/-}$ mice. Paired Student's *t*-test used for statistical analysis.

to increase the specificity of the modified activin B prodomain, we mutated select residues within the α_1 and α_2 helices and the intervening latency lasso, which form the epitopes for growth factor binding. However, no mutations enabled the activin B prodomain to distinguish between the activin isoforms. Interestingly, the generation of a reagent that inhibits only activin A and B may be serendipitous, as recent studies have shown that circulating levels of these growth factors are often coelevated in disease.[28,38] In particular, de Kretser *et al.*[38] demonstrated in a large cohort of acute respiratory failure patients that activin A and B levels are often elevated, and are predictive of the risk of death. These findings, together with the demonstration that activin A and B are produced by many cancer cell lines[25] support the development of the modified activin B prodomain as a therapeutic agent. To this end, we have shown that this reagent can block both activin A and activin B-induced muscle wasting *in vivo*.

The development of activin-specific antagonists also provides an opportunity to uncover novel functions for these growth factors. In this study, we demonstrate for the first time that activin A and activin B contribute to the regulation of muscle homeostasis after birth. While it is clear that myostatin is a major negative regulator of muscle mass (*Mstn*$^{-/-}$ mice have a hypermuscular phenotype associated with increased fiber formation during development and increased fiber size with maturation), many studies have alluded to the involvement of additional TGF-β proteins. For example, the administration of follistatin or soluble ActRIIB to *Mstn*$^{-/-}$ mice results in a further increase in muscle mass,[27,39] and activin A or activin B heterozygous mice present with small increases in musculature.[26] rAAV6-mediated delivery of the modified activin prodomains to the tibialis anterior muscles of normal mice resulted in significant increases (11–14%) in muscle mass, and these increases were further amplified in *Mstn*$^{-/-}$ mice

© The American Society of Gene & Cell Therapy

(17–50%). These findings indicate that activins act in concert with myostatin to negatively regulate muscle mass and that, in the absence of myostatin, the role of activins as negative regulators of muscle mass become more dominant. The inhibitory activity of activins is likely due to circulating forms, as neither activin A nor activin B are well expressed in skeletal muscle. In support, a recent study has determined the normal range for serum activin A (87 ± 4 pg/ml) and activin B (females, 85 ± 5 pg/ml; males, 61 ± 4 pg/ml) in healthy humans aged 18–50 years.[38]

In conclusion, we have for the first time developed the means to specifically inhibit activin isoforms *in vivo*. Future studies will determine whether these reagents can mimic the protective effects of soluble activin type II receptors in disease settings associated with muscle wasting and loss of bone density, without the accompanying off-target effects.

MATERIALS AND METHODS

Generation of modified activin A and B prodomains. The modified activin A and B prodomains were first obtained by PCR targeted to the activin prodomain regions (activin A residues 1–305, activin A sense primer: CTAGTCTAGAATGCCCTTGCTTTGGCTGAGAGG, and antisense primer: CTAGGTTTAAACCTATTTGTCGTCGTCGTCTTTGTAGTC GTGAGG- ATGGTCTTCAGACTGCCTAGCCTG. Activin B residues 1–287, activin B sense primer: CTAGTCTAGAATGGATGGACTTCCA GGTCGAGCTCTGGGGGCCGCCTGCCTTCTGCT-G, and antisense primer: CTAGGCGGCCGCCTATTTGTCGTCGTCGTCTTTGTAGTC GTG- CCTGCTGTCGCCCAG-CCGAGCCTGCACC). The prodomain PCR products were cloned into the *Xba*I and *Not*I sites of the pCDNA3.1(-) plasmid vector (Life Technologies, Carlsbad, CA). The primers incorporated a 3′ FLAG tag. The FLAG-tagged prodomains were subsequently fused to the Fc-domains of a class IgG2A mouse antibody. This was achieved by first amplifying the prodomain regions of activin A and B (activin A sense primer: CTAGGAATTCATGCCCTTGCTTTGG CTGAGAGGATTTC, and antisense primer: CTAGAGATCTTTTGTCG TCGTCGTCTTTGTAGTCGGAG. Activin B sense primer: CTAGG AATTCATGGATGGACTTCCAGGTCGAGCTCTGGG, and antisense primer: CTAGAGATCTTTTGTCGTCGTCGTCTTTGTAGTCGGAG) and cloning the constructs into the *Eco*RI and *Bgl*II sites of pFUSE-mIgG2a-Fc (InvivoGen, San Diego, CA). Finally, the fastener region from the myostatin prodomain (residues 87–94) was substituted into the activin A or B prodomains using overlap-extension PCR (Activin A-fastener sense primer: TTGTTTCCGTTGTAGCGTGATAATCGTCATCCTCT ATCTCCACATACCCGTTCTCCCG-AC, and antisense primer: CGCTAC AACGGAAACAATCATTACCTTTGCCGAG- TCAGGAACAGCCAGG AAGACGC. Activin B-fastener sense primer: GATTATCACGCTAC AACGGAAACAATCATCAGCTTCGCCGAGACAGATG, and antisense primer: GCGTGATAATCGTCATCCTCGATCTCCACGCGGCCG TCCTCGCGC) in combination with flanking primers (detailed above). The prodomain fastener PCR products were then recloned into the *Eco*RI and *Bgl*II sites of pFUSE-mIgG2a-Fc (InvivoGen). For the activin A propeptide, residues in the α_1 helix also involved in formation of the fastener (Asn^{44}/Met^{45}) were replaced with the corresponding Myostatin prodomain residues (Ser^{39}/Lys^{40}) using the QuikChange Lightning mutagenesis kit (Agilent Technologies). This final step was not required for the activin B propeptide, as the corresponding fastener residues are similar to that of Myostatin (Ser^{56}/Arg^{57}).

Production of modified activin A and B prodomains. HEK-293 EBNA cells stably expressing the modified activin A prodomain were revived in DMEM/F12 (Sigma Aldrich, St Louis, MO) supplemented with 10% fetal bovine serum (SAFC, Sigma Aldrich), 2 mg/l puromycin and 300 mg/l G418 (Life Technologies) and seeded into a T-flask. For production, cells were scaled up in Excell293 media (SAFC, Sigma Aldrich) supplemented with 2.5% fetal bovine serum (SAFC, Sigma Aldrich), 2 mg/l puromycin and 300 mg/l G418. Production was carried out in a single use disposable Wave cellbag (GE Healthcare). The culture was fed with the following: 6 g/l Glucose (Sigma Aldrich), 2 mmol/l Glutamax-I (Life Technologies), 5 g/l LucraTone Lupin (Solarbia), 0.2 mmol/l Butyric acid (Sigma Aldrich). To purify the recombinant protein, conditioned media was first centrifuged at 2,975*g* (Beckman Coulter, CA) for 10 minutes, 4 °C and the supernatant clarified using a 0.2 µm filter (Nalgene), the supernatant was loaded onto a protein A Ab-Capcher column (CosmoBio, Japan), and eluted using 0.1 mol/l citrate (pH 3.5) and neutralized with Tris buffer (pH 8.5). Eluted fractions containing the modified activin A prodomain were pooled and concentrated, followed by buffer exchange into PBS (pH 7.2) using a 30 kDa Amicon Ultra centrifugal unit (Merck Millipore, Billerica, MA). Final material was sterile filtered using a 0.2 µm syringe filter (Sartorius, Goettingen, Germany).

The modified activin B prodomain was produced by transient transfection of plasmid DNA into HEK-293F cells using linear polyethylenimine (PEI, 25,000 Mw; BD Biosciences, NJ). The HEK-293F cells were cultured in Freestyle 293 expression medium (Life Technologies) at 37 °C in a humidified atmosphere with 5% CO_2. Posttransfection, the culture was fed with the following: final 6 g/l Glucose (Sigma Aldrich), 2 mmol/l Glutamax-I (Life Technologies), 5 g/l LucraTone Lupin (Solarbia), 0.2 mmol/l Butyric acid (Sigma Aldrich). The culture was harvested by centrifugation at 2,975*g* (Beckman Coulter) for 10 minutes, 4 °C and the supernatant clarified using a 0.2 µm filter (3M Purification). The material was purified as above. The recoveries and yields of the activin prodomains were determined by comparison to FLAG-tagged standards using Western blot analysis (Rabbit anti-FLAG monoclonal antibody; Cell Signaling Technologies) and densitometry with a Chemidoc system (Bio-Rad, Berkeley, CA). The purity of the activin prodomains (typically more than 95%) was assessed by silver stain (Bio-Rad).

Determination of the* in vitro *bioactivity of modified activin A and B prodomains. Two *in vitro* bioassays were used to assess the ability of the modified activin A and B prodomains to block activin signaling. First, mouse pituitary gonadotrope cells (LβT2), which release follicle stimulating hormone (FSH) in response to activin-related ligands, were plated in 48-well plates at a density of 2.5×10^5 cells/well in DMEM media containing 10% FCS and incubated for 24 hours. Cells were washed with DMEM containing 0.2% FCS, and treated with 200 pmol/l of activin A, activin B, myostatin, or GDF-11, and increasing doses of TGF-β antagonists (modified activin A prodomain, modified activin B prodomain, ActRIIA, or ActRIIB) for 24 hours in the same media. FSH levels were determined by a specific rat FSH immunofluorometric assay as previously described[40] employing reagents kindly provided by A Grootenhuis and J Verhagen (N.V. Organon, The Hague, Netherlands).

Alternatively, HEK293F cells were transfected with the Smad2/3-responsive A3-Luciferase reporter construct and FAST2 transcription factor, as previously described,[37] using Lipofectamine 2000 (Life Technologies). At 24 hours posttransfection, cells were treated with recombinant TGF-β1, myostatin, activin A or activin B (R&D Systems, Minneapolis, MN) in the presence of increasing concentration of wild-type or modified prodomains. After 16 hours incubation, cells were harvested in solubilization buffer (1% Triton X-100, 25 mmol/l glycylglycine, pH 7.8, 15 mmol/l $MgSO_4$, 4 mmol/l EGTA, and 1 mmol/l dithiothreitol), and the Smad2/3-induced luciferase activity was determined.

Smad phosphorylation. To assess the capacity of the modified prodomains to suppress activin-mediated signaling, we measured Smad2 phosphorylation via Western blot, in LβT2 cells. Cells were seeded at 2×10^6 cells/well in poly-lysine coated six-well plates. The following day, the media was changed to DMEM, 0.2% FCS and 50 mmol/l HEPES, containing 200 pmol/l activin A/B with increasing concentrations of activin A or

© The American Society of Gene & Cell Therapy

B prodomains (0–60 nmol/l). After 30 minutes of treatment, cells were washed with PBS and lysed in 100 µl RIPA buffer (50 mmol/l Tris-base, 1% Nonidet P-40, 0.5% deoxycholic acid, 0.1% sodium dodecyl sulfate, and 0.9% saline (pH 8.0)), containing protease inhibitor cocktail tablets (Roche Applied Sciences, Penzberg, Germany) and phosphatase inhibitors. Lysates were collected, clarified by centrifugation, and combined with reducing sample buffer (Life Technologies) and analyzed by Western blotting (Bio-Rad). Phospho-Smad2 and Smad2 (Cell Signaling Technologies, Beverly, MA) antibodies were used at 1:2,000 dilutions, respectively. Bound primary antibodies were detected using goat anti-rabbit or sheep anti-mouse horseradish peroxidise conjugates (GE Healthcare Life Sciences, Pittsburgh, PA). These studies were undertaken in three separate replicate cultures.

Production of AAV vectors. cDNA constructs encoding for activin A, activin B, modified activin A prodomain (with 3′ FLAG tag followed by the Fc-domain of a class IgG2A mouse antibody, see **Supplementary Figure 2**), or modified activin B prodomain (with 3′ FLAG tag followed by the Fc-domain of a class IgG2A mouse antibody, see **Supplementary Figure 2**) were cloned into an AAV expression plasmid consisting of a CMV promoter/enhancer and SV40 poly-A region flanked by AAV2 terminal repeats, using standard cloning techniques. These AAV plasmids were cotransfected with pDGM6 packaging plasmid into HEK-293 cells to generate type-6 pseudotyped viral vectors, which were harvested and purified as described previously.[41] Briefly, HEK-293 cells were seeded at $3.2–3.8 \times 10^6$ cells onto a 10 cm culture plate for 8–16 hours prior to transfection. Plates were transfected with 10 µg of a vector-genome-containing plasmid and 20 µg of the packaging/helper plasmid pDGM6, by means of the calcium phosphate precipitate method.[41] After 72 hours, the media and cells were collected and homogenized through a microfluidizer (Microfluidics, Westwood, MA) prior to 0.22 µm clarification (Millipore). Vectors were purified from the clarified lysate by affinity chromatography using HiTrap heparin columns (GE Healthcare), whereupon the elutant was ultracentrifuged overnight, and the vector-rich pellet was resuspended in sterile physiological Ringer's solution. The purified vector preparations were quantified with a customized sequence-specific quantitative PCR-based reaction (Life Technologies).[41]

Animal experiments. All experiments were conducted in accordance with the relevant codes of practice for the care and use of animals for scientific purposes (National Institutes of Health, 1985, and the National Health & Medical Council of Australia, 2013). Vectors carrying transgenes of interest (or control construct) were injected at $10^9 – 1.5 \times 10^{11}$ vg into the *tibialis anterior* (TA) muscles of 6- to 8-week-old male C57BL/6 mice, or 6- to 10-week-old male *Mstn*$^{-/-}$ mice, while the mice were under isoflurane anesthesia. Following vector administration and recovery from anesthesia, mice were monitored until designated endpoints, at which time they were killed humanely via cervical dislocation or CO_2 asphyxiation, and the muscles and organs excised rapidly and weighed before subsequent processing.

Histology. Harvested muscles were placed in OCT cryoprotectant and frozen in liquid nitrogen-cooled isopentane. The frozen samples were cryosectioned at 10 µm thickness and stained with hematoxylin and eosin as described previously.[25] Sections were mounted using DePeX mounting medium (VWR, Leicestershire, UK) and imaged at room temperature using a U-TV1X-2 camera mounted to an IX71 microscope, and an Olympus PlanC 10×/0.25 objective lens. DP2-BSW acquisition software (Olympus) was used to acquire images.

Gene expression profiling and bioinformatics. Gene expression was analyzed in samples of mouse *tibialis anterior* hindlimb muscles collected 7 days after administration of rAAV6:activin A or rAAV6:control as part of a previous study.[25] Total RNA was extracted from frozen muscle via motorized homogenization and purification over RNeasy columns (Qiagen) according to the manufacturer's recommended protocol. RNA quality was determined by the MultiNA capillary electrophoresis system (Shimadzu Biotech, Kyoto, Japan). Messenger RNA was enriched using the NEBNext Poly(A) mRNA Magnetic Isolation Module (New England Biolabs, Ipswich, MA) from 2 µg RNA and sequencing libraries were prepared using the NEBNext mRNA Library Prep Reagent Set for Illumina (New England Biolabs). Libraries were quantified on a MultiNA system and sequenced at a concentration of 12 pmol/l on the Genome Analyzer IIx (Illumina, San Diego, CA). The technical quality of raw sequence data was checked with FastQC. More than [4@3.8M and 2@2.8M 35 nt reads =] 20 million 35-nucleotide-long reads were obtained from six samples from three animals of which >70% aligned uniquely to the mouse genome (mm10) using RNA-star[42] with default settings in Galaxy 43. Reads aligning to exons with a mapping quality score >20 were counted and summed over genes for each sample using HTSeq (EMBL, Heidelberg, http://www-huber.embl.de/users/anders/HTSeq/doc/overview.html). The resulting count matrix was tested for differential gene expression (DGE) between muscles treated with rAAV6:Activin-A and rAAV6:control, including a GLM design term for pairing of case and control legs from each of three animals, using the edgeR Bioconductor package (Fred Hutchinson Cancer Research Centre, http://www.bioconductor.org/packages/2.11/bioc/html/edgeR.html) and false discovery rate control at $P = 0.05$.

Quantitative RT-PCR. Total RNA was collected from TA muscles using TRIzol (Life Technologies). RNA (1–3 µg) was reverse transcribed using the High Capacity RNA-to-cDNA kit (Life Technologies). Expression levels of *Igfn1*, *Mss51*, *Adamts8*, *Mfap4*, *Eln*, and *Comp* were analyzed by quantitative RT-PCR, with 18S to standardize cDNA concentrations, using Taqman assay on-demand kits (Life Technologies) and ABI detection software. For detection of activin A and activin B gene expression, SYBR Green analysis was used (Activin A, Forward primer: GGAGTGTGATGGCAAGGTCAACA, Reverse primer: GTGGGCACA-CAGCATGACTTA. Activin B, Forward primer: GAAGAGTCGCACCGGCCCTTTGTGG, Reverse primer: GAA CTGTTGCCTGCAACAGAGGTTG). 18S was used to standardize cDNA concentrations (Forward primer: GGGAGCCTGAGAAACGGC, Reverse primer: GGGTCGGGAGTGGGTAATTT). Data were analyzed using the ΔΔCT method of analysis and normalized to a control value of 1.

Western blotting. TA muscles were homogenized in RIPA-based lysis buffer (Millipore) supplemented with Phosphatase Inhibitor Cocktails and Protease Inhibitor Cocktails (Sigma Aldrich). Samples were centrifuged at 13,000*g* for 15 minutes at 4 °C and then denatured for 5 minutes at 95 °C. Protein concentration was determined using a protein assay kit (Thermo Scientific, Rockford, IL). Protein fractions were subsequently separated by SDS-PAGE using precast 4–12% Bis-Tris gels (Bio-Rad) blotted onto nitrocellulose membranes (Bio-Rad) and incubated overnight at 4 °C with antibodies against pSmad3 (Epitomics, Burlingame, CA), Smad3 (Epitomics), FLAG (Cell Signaling, Beverly, MA) at 1:1,000 dilution or GAPDH (Santa Cruz Biotechnology, Dallas, TX) at 1:10,000 as described previously,[43] then probed with HRP-conjugated secondary antibody for 1 hour. Chemiluminescence was detected using ECL Western blotting detection reagents (GE Healthcare, Little Chalfont, Buckinghamshire, UK). Quantification of labeled Western blots was performed using ImageJ pixel analysis (US National Institutes of Health, Bethesda, MD). Densitometric analyses of Western blots are presented as band density and normalized to the control value of 1.

Statistical analysis. One-way analysis of variances were used to assess statistical differences across conditions, with the Student-Newman-Keuls *post hoc* test used for comparisons between the specific group means, unless otherwise stated, using GraphPad Prism v.6 (GraphPad, La Jolla, CA). Data columns with different letters achieved significance of $P < 0.05$. Data are presented as the means ± SEM, unless otherwise stated.

© The American Society of Gene & Cell Therapy

SUPPLEMENTARY MATERIAL

Figure S1. Amino acid sequences of myostatin, GDF-11, TGF-β1, TGF-β2, TGF-β3, activin A, and activin B.

Figure S2. Amino acid sequences of the modified (**a**) activin A and (**b**) activin B prodomains (altered residues indicated in bold) fused to Fc domains of mIgG2a (italics).

Figure S3. Potency and specificity of wild-type TGF-β prodomains.

Figure S4. Comparison of first and second generation activin A antagonists.

Figure S5. Activin A and B expression within skeletal muscle.

Table S1. Genes up- or downregulated following 7 day treatment of tibialis anterior muscle with rAAV6:activin A, compared with tibialis anterior muscle receiving empty rAAV6.

ACKNOWLEDGMENTS

Myostatin-null mice were a gift of Se-Jin Lee (Johns Hopkins University, Baltimore, MD). This work was supported by grant funding (526648, 566820) from the National Health and Medical Research Council (NH&MRC, Australia). CAH and PG are supported by NH&MRC Career Development Fellowships (1013533, 1046782 respectively). P.G. was previously supported by a Senior Research Fellowship sponsored by Pfizer Australia. An Endocrine Society of Australia Postdoctoral Fellowship Award supports K.L.W. MIMR-PHI Institute of Medical Research and The Baker IDI Heart & Diabetes Institute are supported in part by the Operational Infrastructure Support Program of the Victorian Government, Australia. The authors declare no conflict of interest.

REFERENCES

1. Makanji, Y, Walton, KL, Chan, KL, Gregorevic, P, Robertson, DM and Harrison, CA (2011). Generation of a specific activin antagonist by modification of the activin A propeptide. *Endocrinology* **152**: 3758–3768.
2. Harrison, CA, Chan, KL and Robertson, DM (2006). Activin-A binds follistatin and type II receptors through overlapping binding sites: generation of mutants with isolated binding activities. *Endocrinology* **147**: 2744–2753.
3. Massagué, J, Seoane, J and Wotton, D (2005). Smad transcription factors. *Genes Dev* **19**: 2783–2810.
4. Cadena, SM, Tomkinson, KN, Monnell, TE, Spaits, MS, Kumar, R, Underwood, KW *et al.* (2010). Administration of a soluble activin type IIB receptor promotes skeletal muscle growth independent of fiber type. *J Appl Physiol* **109**: 635–642.
5. Chantry, AD, Heath, D, Mulivor, AW, Pearsall, S, Baud'huin, M, Coulton, L *et al.* (2010). Inhibiting activin-A signaling stimulates bone formation and prevents cancer-induced bone destruction in vivo. *J Bone Miner Res* **25**: 2633–2646.
6. Lotinun, S, Pearsall, RS, Davies, MV, Marvell, TH, Monnell, TE, Ucran, J *et al.* (2010). A soluble activin receptor Type IIA fusion protein (ACE-011) increases bone mass via a dual anabolic-antiresorptive effect in Cynomolgus monkeys. *Bone* **46**: 1082–1088.
7. Lotinun, S, Pearsall, RS, Horne, WC and Baron, R (2012). Activin receptor signaling: a potential therapeutic target for osteoporosis. *Curr Mol Pharmacol* **5**: 195–204.
8. Pearsall, RS, Canalis, E, Cornwall-Brady, M, Underwood, KW, Haigis, B, Ucran, J *et al.* (2008). A soluble activin type IIA receptor induces bone formation and improves skeletal integrity. *Proc Natl Acad Sci USA* **105**: 7082–7087.
9. Suragani, RN, Cadena, SM, Cawley, SM, Sako, D, Mitchell, D, Li, R *et al.* (2014). Transforming growth factor-ß superfamily ligand trap ACE-536 corrects anemia by promoting late-stage erythropoiesis. *Nat Med* **20**: 408–414.
10. Dussiot, M, Maciel, TT, Fricot, A, Chartier, C, Negre, O, Veiga, J *et al.* (2014). An activin receptor IIA ligand trap corrects ineffective erythropoiesis in ß-thalassemia. *Nat Med* **20**: 398–407.
11. Pistilli, EE, Bogdanovich, S, Goncalves, MD, Ahima, RS, Lachey, J, Seehra, J *et al.* (2011). Targeting the activin type IIB receptor to improve muscle mass and function in the mdx mouse model of Duchenne muscular dystrophy. *Am J Pathol* **178**: 1287–1297.
12. Zhou, X, Wang, JL, Lu, J, Song, Y, Kwak, KS, Jiao, Q *et al.* (2010). Reversal of cancer cachexia and muscle wasting by ActRIIB antagonism leads to prolonged survival. *Cell* **142**: 531–543.
13. Lach-Trifilieff, E, Minetti, GC, Sheppard, K, Ibebunjo, C, Feige, JN, Hartmann, S *et al.* (2014). An antibody blocking activin type II receptors induces strong skeletal muscle hypertrophy and protects from atrophy. *Mol Cell Biol* **34**: 606–618.
14. Fournier, B, Murray, B, Gutzwiller, S, Marcaletti, S, Marcellin, D, Bergling, S *et al.* (2012). Blockade of the activin receptor IIb activates functional brown adipogenesis and thermogenesis by inducing mitochondrial oxidative metabolism. *Mol Cell Biol* **32**: 2871–2879.
15. Gray, AM and Mason, AJ (1990). Requirement for activin A and transforming growth factor–beta 1 pro-regions in homodimer assembly. *Science* **247**: 1328–1330.
16. Harrison, CA, Al-Musawi, SL and Walton, KL (2011). Prodomains regulate the synthesis, extracellular localisation and activity of TGF-ß superfamily ligands. *Growth Factors* **29**: 174–186.
17. Walton, KL, Makanji, Y, Chen, J, Wilce, MC, Chan, KL, Robertson, DM *et al.* (2010). Two distinct regions of latency-associated peptide coordinate stability of the latent transforming growth factor-beta1 complex. *J Biol Chem* **285**: 17029–17037.
18. Annes, JP, Munger, JS and Rifkin, DB (2003). Making sense of latent TGFbeta activation. *J Cell Sci* **116**(Pt 2): 217–224.
19. Ge, G, Hopkins, DR, Ho, WB and Greenspan, DS (2005). GDF11 forms a bone morphogenetic protein 1-activated latent complex that can modulate nerve growth factor-induced differentiation of PC12 cells. *Mol Cell Biol* **25**: 5846–5858.
20. Wolfman, NM, McPherron, AC, Pappano, WN, Davies, MV, Song, K, Tomkinson, KN *et al.* (2003). Activation of latent myostatin by the BMP-1/tolloid family of metalloproteinases. *Proc Natl Acad Sci USA* **100**: 15842–15846.
21. Shi, M, Zhu, J, Wang, R, Chen, X, Mi, L, Walz, T *et al.* (2011). Latent TGF-ß structure and activation. *Nature* **474**: 343–349.
22. Böttinger, EP, Factor, VM, Tsang, ML, Weatherbee, JA, Kopp, JB, Qian, SW *et al.* (1996). The recombinant proregion of transforming growth factor beta1 (latency-associated peptide) inhibits active transforming growth factor beta1 in transgenic mice. *Proc Natl Acad Sci USA* **93**: 5877–5882.
23. Matsakas, A, Foster, K, Otto, A, Macharia, R, Elashry, MI, Feist, S *et al.* (2009). Molecular, cellular and physiological investigation of myostatin propeptide-mediated muscle growth in adult mice. *Neuromuscul Disord* **19**: 489–499.
24. Qiao, C, Li, J, Jiang, J, Zhu, X, Wang, B, Li, J *et al.* (2008). Myostatin propeptide gene delivery by adeno-associated virus serotype 8 vectors enhances muscle growth and ameliorates dystrophic phenotypes in mdx mice. *Hum Gene Ther* **19**: 241–254.
25. Chen, JL, Walton, KL, Winbanks, CE, Murphy, KT, Thomson, RE, Makanji, Y *et al.* (2014). Elevated expression of activins promotes muscle wasting and cachexia. *FASEB J* **28**: 1711–1723.
26. Lee, SJ, Lee, YS, Zimmers, TA, Soleimani, A, Matzuk, MM, Tsuchida, K *et al.* (2010). Regulation of muscle mass by follistatin and activins. *Mol Endocrinol* **24**: 1998–2008.
27. Lee, SJ, Reed, LA, Davies, MV, Girgenrath, S, Goad, ME, Tomkinson, KN *et al.* (2005). Regulation of muscle growth by multiple ligands signaling through activin type II receptors. *Proc Natl Acad Sci USA* **102**: 18117–18122.
28. Li, Q, Kumar, R, Underwood, K, O'Connor, AE, Loveland, KL, Seehra, JS *et al.* (2007). Prevention of cachexia-like syndrome development and reduction of tumor progression in inhibin-deficient mice following administration of a chimeric activin receptor type II-murine Fc protein. *Mol Hum Reprod* **13**: 675–683.
29. Jones, KL, Mansell, A, Patella, S, Scott, BJ, Hedger, MP, de Kretser, DM *et al.* (2007). Activin A is a critical component of the inflammatory response, and its binding protein, follistatin, reduces mortality in endotoxemia. *Proc Natl Acad Sci USA* **104**: 16239–16244.
30. Munz, B, Smola, H, Engelhardt, F, Bleuel, K, Brauchle, M, Lein, I *et al.* (1999). Overexpression of activin A in the skin of transgenic mice reveals new activities of activin in epidermal morphogenesis, dermal fibrosis and wound repair. *EMBO J* **18**: 5205–5215.
31. Vale, W, Rivier, C, Hsueh, A, Campen, C, Meunier, H, Bicsak, T *et al.* (1988). Chemical and biological characterization of the inhibin family of protein hormones. *Recent Prog Horm Res* **44**: 1–34.
32. Xia, Y and Schneyer, AL (2009). The biology of activin: recent advances in structure, regulation and function. *J Endocrinol* **202**: 1–12.
33. David, L, Mallet, C, Mazerbourg, S, Feige, JJ and Bailly, S (2007). Identification of BMP9 and BMP10 as functional activators of the orphan activin receptor-like kinase 1 (ALK1) in endothelial cells. *Blood* **109**: 1953–1961.
34. Morris, C (2013). Balancing Efficacy versus safety: learnings from development of myostatin inhibitiors. *DACC News* **29**: 8.
35. Al-Musawi, SL, Walton, KL, Heath, D, Simpson, CM and Harrison, CA (2013). Species differences in the expression and activity of bone morphogenetic protein 15. *Endocrinology* **154**: 888–899.
36. Simpson, CM, Stanton, PG, Walton, KL, Chan, KL, Ritter, LJ, Gilchrist, RB *et al.* (2012). Activation of latent human GDF9 by a single residue change (Gly 391 Arg) in the mature domain. *Endocrinology* **153**: 1301–1310.
37. Walton, KL, Makanji, Y, Wilce, MC, Chan, KL, Robertson, DM and Harrison, CA (2009). A common biosynthetic pathway governs the dimerization and secretion of inhibin and related transforming growth factor beta (TGFbeta) ligands. *J Biol Chem* **284**: 9311–9320.
38. de Kretser, DM, Bensley, JG, Pettilä, V, Linko, R, Hedger, MP, Hayward, S *et al.* (2013). Serum activin A and B levels predict outcome in patients with acute respiratory failure: a prospective cohort study. *Crit Care* **17**: R263.
39. Lee, SJ (2007). Quadrupling muscle mass in mice by targeting TGF-beta signaling pathways. *PLoS ONE* **2**: e789.
40. Makanji, Y, Harrison, CA, Stanton, PG, Krishna, R and Robertson, DM (2007). Inhibin A and B *in vitro* bioactivities are modified by their degree of glycosylation and their affinities to betaglycan. *Endocrinology* **148**: 2309–2316.
41. Blankinship, MJ, Gregorevic, P, Allen, JM, Harper, SQ, Harper, H, Halbert, CL *et al.* (2004). Efficient transduction of skeletal muscle using vectors based on adeno-associated virus serotype 6. *Mol Ther* **10**: 671–678.
42. Dobin, A, Davis, CA, Schlesinger, F, Drenkow, J, Zaleski, C, Jha, S *et al.* (2013). STAR: ultrafast universal RNA-seq aligner. *Bioinformatics* **29**: 15–21.
43. Winbanks, CE, Wang, B, Beyer, C, Koh, P, White, L, Kantharidis, P *et al.* (2011). TGF-beta regulates miR-206 and miR-29 to control myogenic differentiation through regulation of HDAC4. *J Biol Chem* **286**: 13805–13814.